Marine Energy Research

SciEPublish

Article

Mooring Material Cost Estimation for a Floating Photovoltaic Farm

Shan Wang *, Hao Jiang, Afonso Santos, Sara Ramos-Marin and Carlos Guedes Soares

Centre for Marine Technology and Ocean Engineering (CENTEC), Instituto Superior Tecnico, Universidade de Lisboa, 1049-001 Lisbon, Portugal; hao.jiang@tecnico.ulisboa.pt (H.J.); afonso.c.g.a.santos@tecnico.ulisboa.pt (A.S.); sara.ramos@centec.tecnico.ulisboa.pt (S.R.-M.); c.guedes.soares@centec.tecnico.ulisboa.pt (C.G.S.)

* Corresponding author. E-mail: shan.wang@centec.tecnico.ulisboa.pt (S.W.)

Received: 30 September 2026; Revised: 28 October 2026; Accepted: 3 November 2026; Available online: 25 November 2026

ABSTRACT: This study presents mooring material cost estimates for two floating photovoltaic concepts developed in NATURSEA-PV at different potential sites. Based on the quasi-static mooring model and the three-component chain–polyester–chain configuration developed in the previous study, a cost-based optimisation is performed for selected sites in the Algarve, Canary Islands and Adriatic Sea. The total mooring line length, polyester length and initial pretension are optimised while satisfying the prescribed requirements for maximum mooring tension, platform offset and seabed contact. The estimated cost includes the chain, polyester rope and anchors, with the anchor cost determined according to the anchor force. The optimisation is performed for two substructure designs, and the resulting costs are compared at both unit and farm levels. The results show that water depth and the associated mooring line length are the main factors governing the material cost, while differences in environmental conditions mainly influence the tension utilisation and platform offset. The two designs generally result in comparable mooring costs per floating unit. However, Design 2, with a larger span between the floaters, requires fewer floating units at farm level and therefore results in approximately 40.5–49.4% lower total mooring cost than Design 1 for the comparable sites considered.

Keywords: Offshore floating photovoltaic system; Mooring analysis; Cost evaluation; Optimization

1. Introduction

Floating photovoltaic (FPV) systems have developed rapidly in recent years as an alternative to conventional land-based photovoltaic installations, particularly in regions with limited land availability. In addition to reducing competition for land, floating deployment can benefit from the cooling effect of water and provide opportunities for large-scale renewable energy production close to highly populated coastal regions [1–3]. Most existing FPV installations, however, are located in reservoirs, lakes, and other sheltered water bodies. Extending the technology towards nearshore and offshore environments introduces substantially more demanding environmental and structural conditions, including larger waves, stronger winds and currents, corrosion and cyclic loading [2,4]. The design of the floating structure and its mooring system therefore becomes increasingly important for ensuring the survivability and economic competitiveness of offshore floating photovoltaic (OFPV) systems.

© 2026 The authors. This is an open access article under the Creative Commons Attribution 4.0 International License (https://creativecommons.org/licenses/by/4.0/).

For OFPV systems, the mooring system must provide sufficient restoring capacity while maintaining a relatively low cost per unit. Its design is also strongly site-dependent. Water depth directly affects the required line geometry and material quantity, whereas waves, wind, and currents determine the platform offset, mooring tension, and required anchor capacity. These effects become increasingly important at farm level, where the mooring system is repeated over a large number of floating units. Several studies have investigated mooring concepts for FPV systems. Yu et al. [5] analysed the dynamic response of the mooring system of an FPV power station in relatively shallow and sheltered water. Ghigo et al. [6] investigated an offshore FPV concept for the island of Lampedusa using four catenary lines made of R3 studless chain connected to drag-embedded anchors. These existing studies have considered different catenary, taut, and hybrid mooring arrangements for floating renewable energy systems. Nevertheless, most studies on FPV moorings have concentrated on structural response or the performance of a particular mooring configuration under prescribed environmental conditions.

The selection of the mooring material is another important aspect of the design. Synthetic fibre ropes provide an alternative to conventional chain and wire systems because of their relatively low submerged weight, high strength, and compliant characteristics. Weller et al. [7] reviewed synthetic ropes for marine renewable energy applications and identified their potential for economical and reliable station-keeping systems. Xu et al. [8] reviewed mooring designs for floating wave energy converters and showed that elastic synthetic ropes and hybrid mooring systems can provide attractive solutions depending on the characteristics of the floating device. Experimental investigations by Xu et al. [9] further demonstrated that the selection of rope material significantly affects the dynamic response and fatigue behaviour of moored floating systems. These studies support using multi-component mooring lines that combine conventional chain and synthetic fibre ropes for offshore renewable energy applications. More recently, attention has shifted from assessing individual mooring configurations to systematic optimisation. Han et al. [10] developed an integrated coupling and multi-objective optimisation framework for FPV arrays, combining static screening, dynamic analysis and surrogate-based optimisation. Their study demonstrated that systematic optimisation could improve the cost efficiency of FPV mooring systems while satisfying the required structural performance.

The economic performance of the mooring system is particularly relevant for offshore renewable energy technologies, for which reducing the levelised cost of energy (LCOE) remains an important requirement for large-scale commercial deployment [11]. Thomsen et al. [12] performed cost optimisation of mooring solutions for large floating wave energy converters and demonstrated the importance of considering cost alongside structural requirements when selecting mooring configurations. Housner et al. [13] investigated shared mooring systems for WEC arrays and demonstrated substantial reductions in the mooring cost per device compared with individual mooring systems. In particular, the 2 × 3 array considered in their study achieved a 60% reduction in mooring cost per WEC, while reductions of approximately 50% were obtained for the 3 × 3 and 4 × 4 arrays [13]. These studies demonstrate that mooring optimisation becomes increasingly important when floating renewable energy devices are deployed at farm scale. More generally, the economic assessment of floating offshore renewable energy farms requires the different life cycle cost components to be considered together. Castro-Santos et al. [14] developed a methodology for estimating the costs of floating offshore renewable energy farms, accounting for the main stages of the project life cycle.

Similar economic considerations have been applied to floating offshore wind. Castro-Santos et al. [15] assessed the economic feasibility of floating offshore wind farms in Portugal, illustrating the importance of site and project characteristics in determining their economic performance. Myhr et al. [16] investigated the LCOE of several floating wind concepts from a life cycle perspective and showed that the resulting LCOE is strongly dependent on water depth and distance from shore. In particular, the influence of water depth was associated with variations in the mooring cost, while distance from shore affected the export

cable cost. Lerch et al. [17] subsequently performed a comprehensive sensitivity analysis for floating offshore wind farms and identified the manufacturing costs of the turbine, substructure, and mooring system, together with the power cable cost, as parameters influencing LCOE. These studies show that the station-keeping system represents not only a structural design issue but also an important component in the economic optimisation of floating offshore renewable energy systems.

Economic studies specifically addressing OFPV remain relatively limited compared with floating wind and wave energy, although several recent investigations have begun to quantify its cost competitiveness. Martinez and Iglesias [18] mapped the LCOE of floating solar PV in the coastal waters of the European Atlantic, North Sea and Baltic Sea. Their results showed substantial geographical variations in LCOE, with latitude and distance to the coast identified as the dominant parameters and water depth having a secondary influence. The lowest LCOE values, approximately 250 EUR/MWh, were obtained in nearshore waters off southwestern Spain and Portugal [18]. Their results also showed considerably higher values in other regions, reaching approximately 650 EUR/MWh in northern Norway. A more detailed life cycle cost analysis was recently performed by Bru et al. [19] for an offshore FPV concept at two sites in the North Sea. The estimated LCOE was 256.7 EUR/MWh for Sørlige Nordsjø II and 287 EUR/MWh for Utsira Nord. Their analysis considered a 25-year project lifetime and a discount rate of 6%, and also investigated the sensitivity and uncertainty of the estimated LCOE. Results showed that economic performance depends strongly on the project and site characteristics, including energy production, grid distance, lifetime, and discount rate. These recent studies demonstrate the importance of site-dependent economic assessment for OFPV and indicate that further cost reduction is required to improve its competitiveness.

Within the NATURSEA PV project, a three-component mooring configuration consisting of an upper chain, polyester rope, and lower chain was developed for the proposed offshore floating PV concept [20]. Static and quasi-static analyses were initially performed to investigate alternative mooring configurations [21], followed by fully coupled dynamic simulations under extreme environmental conditions [22] at the potential area [23]. In parallel, a GIS-based spatial screening assessment was conducted for three representative European marine regions: the Algarve, Canary Islands, and Adriatic Sea, to identify areas potentially suitable for OFPV deployment considering resource, engineering, geological, environmental, and marine spatial-planning constraints [24]. Representative locations within the resulting suitable areas were then characterised in terms of water depth and site-specific metocean conditions to support subsequent structural and mooring assessments.

The present study develops a site-dependent cost optimisation framework for two OFPV platform concepts using the environmental conditions obtained for the selected deployment locations. A quasi-static mooring analysis is coupled with a derivative-free pattern search algorithm to optimise the total mooring line length, polyester segment length and initial pretension while satisfying the prescribed requirements for maximum tension, platform offset and seabed contact. The optimisation is applied consistently across the selected sites and the two platform concepts to quantify how site-specific conditions affect the resulting mooring configuration, structural response, and material cost. Finally, the two platform concepts are compared at both individual unit and farm levels, providing a direct link between site-dependent mooring design and the economic assessment of large scale OFPV deployment. Although the LCOE is not calculated directly in the present study, the resulting mooring costs provide an important input for subsequent LCOE assessments.

2. Methodology

The methodology developed in this study combines quasi-static mooring analysis with cost-based optimisation to determine the mooring configuration for each floating platform and deployment site [25,26]. The overall procedure for the quasi-static analysis is illustrated in Figure 1. The platform characteristics, mooring material properties and site-specific environmental conditions are first defined as input. A three-component mooring line consisting of an upper chain, polyester rope, and lower chain is adopted as the

reference configuration. The total mooring line length, polyester segment length and initial horizontal pretension are selected as the design variables, while the line diameters and material properties remain unchanged throughout the optimisation.

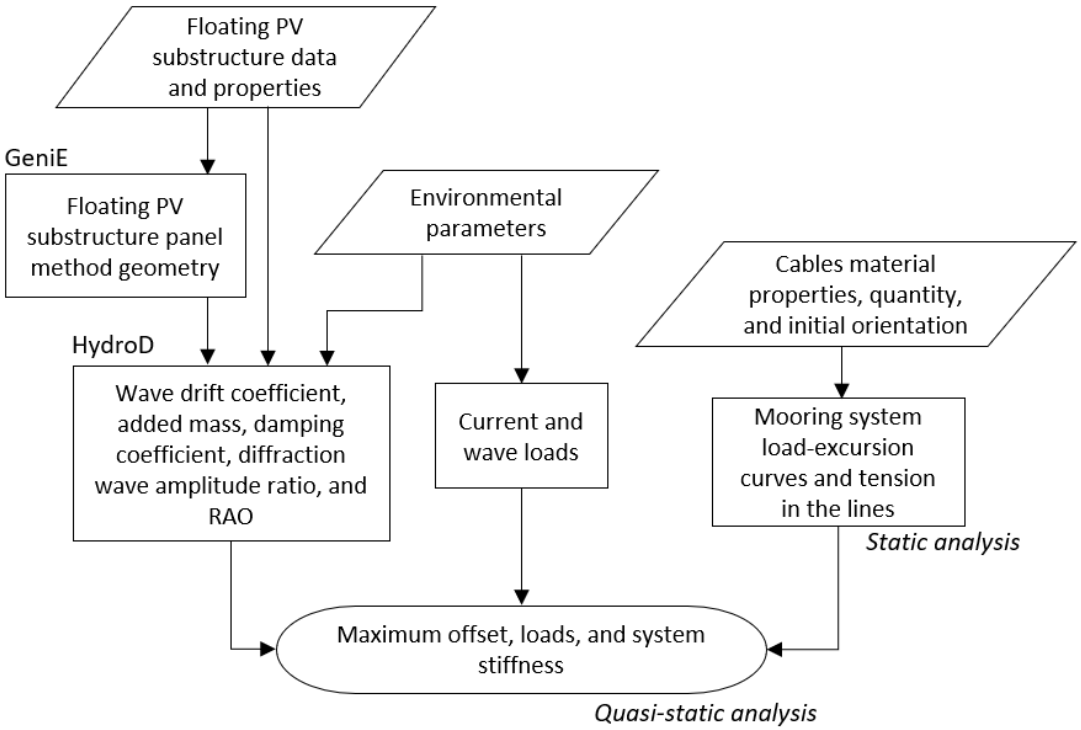

Figure 1. Flowchart of the calculation procedure for the quasi-static analysis.

For each candidate design, a static analysis is first performed to determine the equilibrium configuration of the mooring lines and establish the restoring force as a function of platform horizontal displacement. The mean environmental load is then calculated by considering the contributions from wind, current, and mean wave drift. The corresponding mean platform offset is obtained from the intersection between the environmental load and the mooring restoring force. The local mooring stiffness at the mean equilibrium position is subsequently used in quasi-static analysis to estimate the wave frequency surge response. The maximum platform excursion is determined by combining the mean offset and the estimated maximum wave frequency surge amplitude. The corresponding maximum mooring tension and seabed contact condition are then evaluated.

The calculated mooring response is checked against the prescribed design requirements for maximum line tension, platform offset, and seabed contact. Configurations satisfying all the requirements are considered feasible, and their material and anchor costs are evaluated. A derivative free pattern search algorithm is then used to vary the design variables and identify the feasible configuration with the minimum estimated mooring cost. The same procedure is applied independently to the selected sites and to both floating platform concepts. Finally, the optimised costs per floating unit are scaled according to the required number of units to evaluate and compare the mooring costs at farm level.

The present method is implemented in MATLAB following the criteria below:

- The calculated maximum tension (T_{max}), multiplied by a safety factor γ = 1.67 from DNV-OS-E301 [27], must result in less than 0.95 times the minimum breaking strength (T_{br}) of the cable;
- Slack should not occur in the mooring lines, as this condition can potentially lead to large snap tension loads;

- The synthetic fibre ropes should not be in contact with the seabed and floater to avoid abrasion of the synthetic fibres;
- The length of the lifted cable must be lower than the length of the cable to maintain catenary configuration;
- The offset is limited to a reasonable range to avoid excessive damage to power cables.

2.1. Static Mooring Analysis

The static analysis uses elastic catenary equations to determine the equilibrium configuration and tension distribution of the mooring lines under static conditions, assuming a horizontal seabed. For the three-component line shown in Figure 2, the suspended portions of the upper chain, polyester rope, and lower chain are treated as individual segments. The horizontal tension component H is constant along the line, whereas the vertical tension varies with the submerged weight of each segment. Elasticity of the polyester rope is included through its axial stiffness EA.

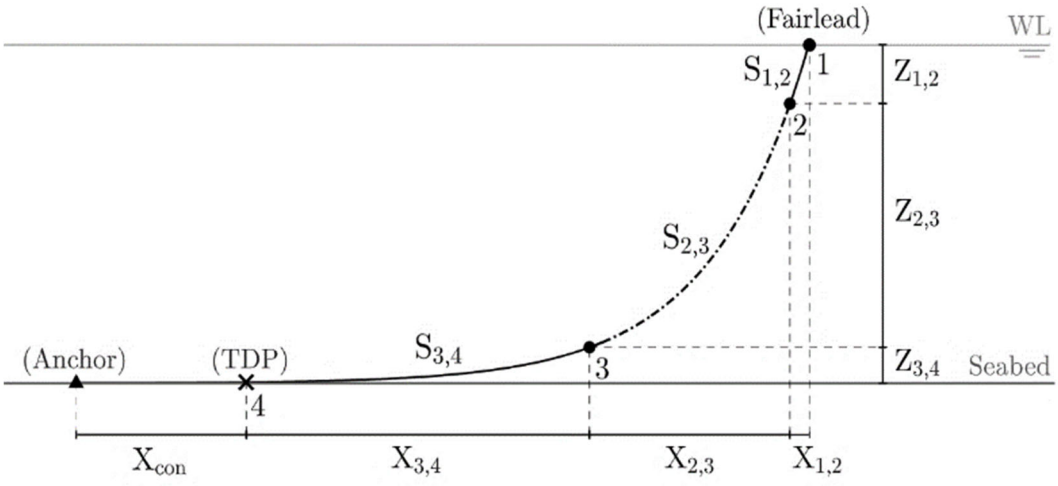

Figure 2. Representation of the three-component cable parameters for the catenary solution.

For a segment between points i and $i + 1$, the vertical force and the horizontal and vertical projections of the suspended line are given by

$$V_{i,i+1}(s) = V_{i+1} + w_i S_{i,i+1}(s), i = 1, 2, 3 \tag{1}$$

$$X_{i,i+1} = \frac{H}{w_i}\left[sinh^{-1}\left(\frac{V_i}{H}\right) - sinh^{-1}\left(\frac{V_{i+1}}{H}\right)\right] + \frac{H(V_i - V_{i+1})}{w_i EA_i}, i = 1, 2, 3 \tag{2}$$

$$Z_{i,i+1} = \frac{H}{w_j}\left[\sqrt{1 + \left(\frac{V_i}{H}\right)^2} - 1 + \left(\frac{V_{i+1}}{H}\right)^2\right] + \frac{V_i^2 - V_i^2}{2w_i EA_i}, i = 1, 2, 3 \tag{3}$$

where $V_{i,i+1}(s)$ is the vertical component of tension along the segment, w_i is the submerged weight per unit length, $S_{i,i+1}(s)$ is the suspended segment length, H is the horizontal component of tension, $X_{i,i+1}$ and $Z_{i,i+1}$ are the horizontal and vertical projections, respectively, and EA_i is the axial stiffness of the segment.

For the three-component line, the vertical projections must satisfy the water-depth condition.

$$Z_{1,2} + Z_{2,3} + Z_{3,4} = h \tag{4}$$

and the total horizontal anchor-to-fairlead distance is obtained from

$$X_{1,2} + X_{2,3} + X_{3,4} + X_{con} = X_L \tag{5}$$

where X_{con} is the horizontal distance between the anchor and the touchdown point.

The solution is obtained iteratively. For a prescribed horizontal pretension, the vertical force at the fairlead is varied until the sum of the vertical projections equals the fairlead-to-seabed distance. The horizontal projections of the suspended segments and the seabed portion of the lower chain then provide the total anchor-to-fairlead distance. Repeating the static solution for a range of platform excursions gives the nonlinear restoring-force versus excursion curve and the corresponding fairlead, polyester and anchor tensions.

2.2. Quasi-Static Response

The quasi-static analysis combines the restoring characteristics obtained from the static analysis with the environmental loads. Wind, current, and mean wave-drift loads are treated as mean environmental loads, while the wave-frequency response is superimposed to estimate the maximum surge offset. Low-frequency loads are neglected in the present screening model. The wind and current loads follow DNV-RP-C205 [28], and the details can be found in ref. [21].

The mean wave-drift force is calculated using the diagonal wave-drift coefficient $P(\omega,\omega)$ obtained from HydroD V9.0-01 and the wave spectrum $S_w(\omega)$:

$$F_{Drift} = 2\int S_w(\omega)\cdot P(\omega,\omega)\, d\omega \tag{6}$$

The wave-frequency load is evaluated from the diffraction-force amplitude ratio obtained from HydroD. The corresponding force spectrum is

$$S_F(\omega) = \left(f_{wd}(\omega)\right)^2 S_w(\omega) \tag{7}$$

and the significant wave-force amplitude is obtained from the spectral integral:

$$F_{sig} = 2\sqrt{\int S_F(\omega)d\omega} \tag{8}$$

The mean surge offset, δ_{mean}, is obtained by balancing the mean environmental force with the nonlinear restoring-force curve. The local mooring stiffness at this equilibrium position is taken as the slope of the restoring curve and is used together with the platform hydrodynamic coefficients to estimate the wave-frequency surge response. The surge response spectrum is expressed as

$$S_x(\omega) = \frac{S_F(\omega)}{(S-(M+M_a)\omega^2)^2 + b^2\omega^2} \tag{9}$$

where S is the local mooring stiffness at the mean offset, M is the platform mass, M_a is the surge added mass, and b is the radiation damping coefficient. The added mass, radiation damping, and wave-excitation coefficients are obtained from HydroD V9.0-01. The significant and maximum wave-frequency surge amplitudes are calculated as

$$x_{sig} = 2\sqrt{\int S_x(\omega)\ d\omega} \tag{10}$$

$$x_{max} = 1.9x_{sig} \tag{11}$$

In the present implementation, the maximum horizontal offset is obtained by adding the maximum wave-frequency surge amplitude to the mean offset. The maximum fairlead, polyester, and anchor tensions are then interpolated from the static response curves at this maximum excursion.

The design checks require the maximum line tension, multiplied by the safety factor, to remain below 95% of the minimum breaking load; the platform offset to remain within the prescribed limit. In addition, the lower chain maintains the required seabed-contact condition so that the polyester segment remains clear of the seabed. The tension requirement can be written as

$$T_{max} \times \gamma < 0.95 \times T_{Br} \tag{12}$$

2.3. Cost-Based Mooring Optimisation

The mooring cost estimation follows the material cost equations from Housner et al. [13], in which the costs of chain, polyester rope and anchors are estimated separately. The unit costs of chain and polyester rope are expressed as functions of their nominal diameters, while the anchor cost is estimated from the maximum anchor load. The cost coefficients are taken directly from ref. [13] and are applied to both platform concepts and all selected sites.

Based on the static and quasi-static mooring model described above, a cost-based optimisation framework is developed to determine the mooring configuration for each installation site. The mooring material properties and dimensions were prescribed, while the line geometry and pretension were optimised. To enable a consistent optimisation procedure for sites with different water depths, three non-dimensional design variables were introduced:

$$x = [L_{tot}/h, L_{poly}/L_{tot}, H_0/MBL] \tag{13}$$

where L_{tot} is the total length of one mooring line, h is the water depth, L_{poly} is the length of the polyester segment, H_0 is the initial horizontal pretension, and MBL is the minimum breaking load of the mooring line. Accordingly, the dimensional design parameters are obtained as

$$L_{tot} = x_1 \cdot h \tag{14}$$

$$L_{poly} = x_2 \cdot L_{tot} \tag{15}$$

$$H_0 = x_3 \cdot MBL \tag{16}$$

The length of the upper chain segment, L_{top}, was fixed at 15 m and was therefore excluded from the optimisation. Once the total line length and polyester length were determined, the length of the lower chain segment was calculated as

$$L_{bottom} = L_{tot} - L_{top} - L_{poly} \tag{17}$$

The objective of the optimisation was to minimise the estimated mooring-system cost, including the chain, polyester rope and anchors, while satisfying the prescribed design requirements. For a system consisting of N_{line} identical mooring lines, the objective function was defined as ref. [13].

$$C_{total} = Nline \times (c_{chain} \cdot L_{chain} + c_{fiber} \cdot L_{fiber} + C_{anchor}) \tag{18}$$

where c_{chain} and c_{fiber} represent the unit cost per meter of the respective line materials, L_{chain} and L_{fiber} denote their total lengths, and C_{anchor} is the procurement cost of the anchors.

The unit costs for mooring lines are modeled as a function of the material volume per meter, which correlates directly with the square of the nominal diameter (d^2). This quadratic relationship aligns with offshore industry procurement standards, where manufacturing and raw material costs are proportional to the mass and cross-sectional area of the components. Specifically, the unit cost for high-strength steel chain is established at c_{chain} = (51,440/m^3)·d^2. This coefficient inherently accounts for the manufacturing complexity of offshore-grade chains, including the high-quality steel alloys required to withstand severe marine corrosion and fatigue loading over a 25-year service life. For the compliant fiber segments (e.g., Type P4), the unit cost is formulated as c_{fiber} = (2810/m^3) ·d^2. The significantly lower volume-based cost coefficient reflects the lower material density and different extrusion processes compared to forged steel, making synthetic ropes a critical component for deep-water economic optimization.

Furthermore, the procurement cost of drag-embedment anchors (C_{anchor}) is strictly modeled based on the required holding capacity. This capacity is directly determined by the maximum dynamic tension at the

anchor point (T_{anc_max}), which is extracted from the Upper Bound quasi-static analysis (Pass 2) to simulate the most extreme storm conditions. To ensure conservative economic planning and adhere to offshore safety regulations, a dynamic safety multiplier of 1.5 is applied to the maximum load:

$$C_{anchor} = (\$0.188/\text{kg}) \cdot \frac{T_{anc_max} \times 1.5}{g} \tag{19}$$

where g is the acceleration due to gravity.

For each candidate configuration, the mooring response was evaluated using the method described in the previous section. The maximum mooring-line tension, maximum horizontal platform offset, and seabed-contact condition of the lower chain were considered as design constraints. The tension constraint was expressed in terms of the utilisation ratio as

$$Tmax/MBL \leq R_{Tlim} \tag{20}$$

where T_{max} is the maximum line tension. An allowable tension ratio of $R_{Tlim} = 0.95/1.67 = 0.569$ was adopted. The maximum horizontal offset was normalised by the local water depth and constrained according to

$$\delta max/h \leq R\delta lim \tag{21}$$

where δ_{max} denotes the maximum horizontal displacement of the floating structure and $R_{\delta lim} = 0.25$. In addition, the lower chain was required to satisfy the prescribed seabed-contact condition to avoid configurations with insufficient chain remaining on the seabed.

The resulting optimisation problem can therefore be expressed as

$$min_x\, C(x) \tag{22}$$

$$Tmax(x)/MBL \leq 0.569 \tag{23}$$

$$\delta max(x)/h \leq 0.25 \tag{24}$$

$$L_{bottom}, seabed(x) \geq L_{seabed}, min \tag{25}$$

$$x_L \leq x \leq x_U \tag{26}$$

where x_L and x_U denote the lower and upper bounds of the design variables, respectively.

A derivative-free pattern-search algorithm [29] is employed to solve the constrained optimisation problem. This approach is suitable for the present application because the evaluation of the objective and constraint functions involves nonlinear mooring responses, changes in seabed contact, and iterative equilibrium calculations, for which analytical gradients are not readily available.

Starting from an initial design, the algorithm evaluates neighbouring candidate solutions within the prescribed design space and progressively adjusts the search mesh according to the improvement of the objective function and the satisfaction of the design constraints. The optimisation terminates when the prescribed convergence criteria are reached, or the maximum number of function evaluations is exceeded.

The same optimisation framework, objective function and design constraints were applied to all installation sites and two designs of the floating substructure, allowing their optimised mooring configurations and associated material costs to be compared on a consistent basis. The bounds of L_{tot}/h were adjusted according to the water depth to accommodate the geometric requirements of shallow- and deep-water mooring systems, while the ranges of the polyester-length ratio and pretension ratio were kept consistent.

3. Description of the OFPV System and Potential Sites

3.1. Substructure and Mooring Systems

Two offshore floating photovoltaic substructure concepts developed within the NATURSEA PV project are considered in the present study. The concepts are based on a modular orthogonal arrangement of floaters and connecting beams, selected during the conceptual design stage for its relatively simple configuration and potential construction and cost advantages compared with the initially proposed lily-shaped arrangement [30]. The subsequent structural design was developed using precast ultra-high-performance concrete (UHPC) components, with the dimensions and arrangement adapted to different levels of environmental severity [31]. Figure 3 shows the recommended designs of the structure.

Design 1 is intended for relatively harsh offshore environments and was developed to maintain the PV panels above the water surface for wave heights up to approximately 14 m. The design adopts a relatively compact arrangement with a characteristic spacing of 6 m between adjacent floaters. The original predesign consists of 21 floaters connected by 36 beams at two structural levels. Design 2 is intended for intermediate offshore conditions, with the corresponding structural design developed for wave heights up to approximately 7 m. The spacing between adjacent floaters is increased to 11 m, allowing a larger area to be supported by each floating unit while maintaining the same general structural concept.

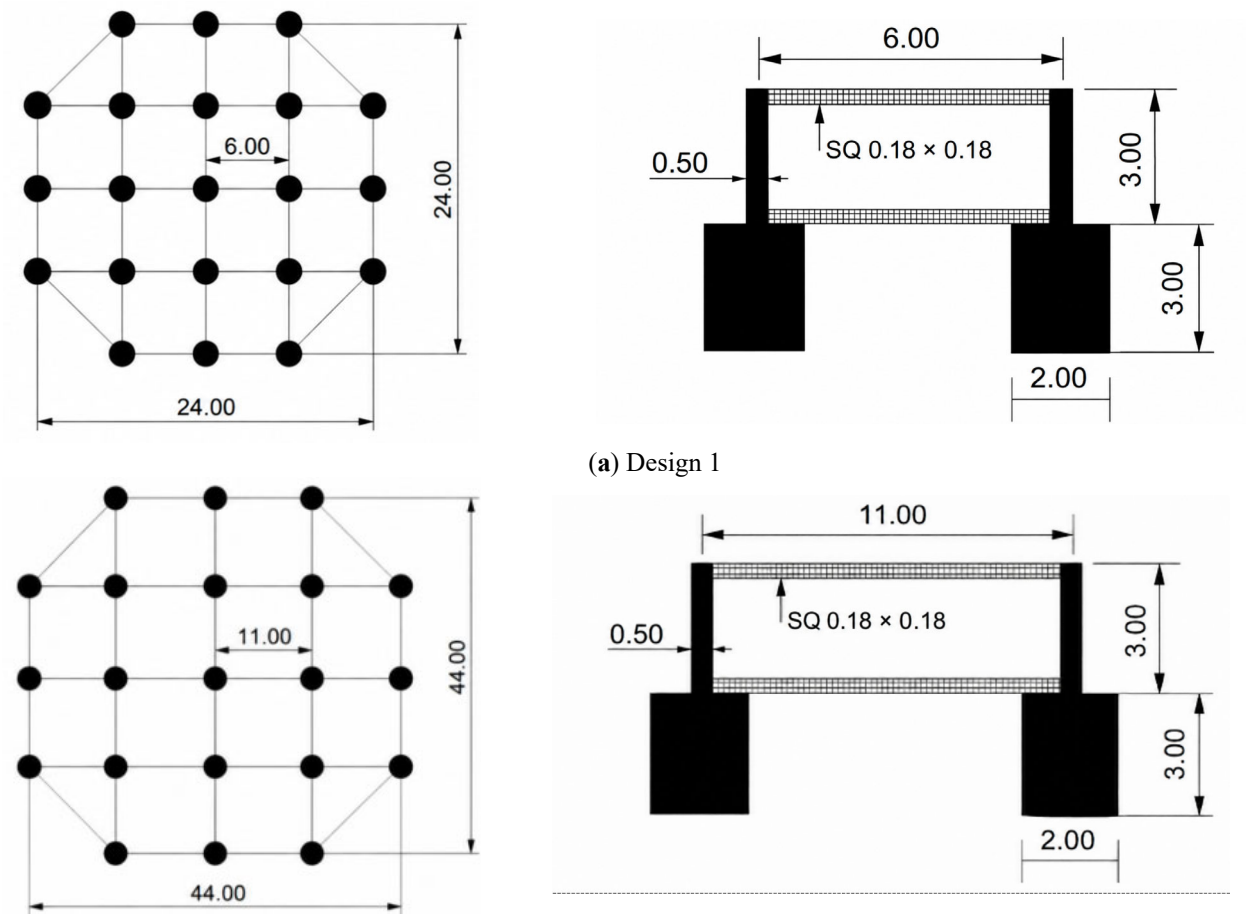

Figure 3. Recommended design of the substructure (unit: m) [31] (**a**) Design 1; (**b**) Design 2.

Design 2 adopts larger structural spans for less severe conditions. The larger spacing in Design 2 reduces the number of floating units required to cover a given farm area, which is particularly relevant when mooring cost is evaluated at the farm level. In the present study, the two concepts are therefore assessed using the same mooring optimisation framework, allowing the effects of platform characteristics

and the number of required floating units on both unit and farm level mooring costs to be compared. The main geometrical differences are the spacing between adjacent floaters, which increases from 6 m in Design 1 to 11 m in Design 2, and the draft, which increases from 1.85 m to 2.35 m, respectively.

The mooring system consists of four three-component mooring lines, with a polyester rope segment connected to upper and lower chain segments, as shown in Figure 4. The main material properties are kept unchanged for all sites and for both Design 1 and Design 2, while the total line length, polyester length, and initial pretension are varied during the optimisation.

The main properties adopted in the present analysis are summarised in Table 1. The chain and polyester diameters and their mechanical properties [32,33] are fixed throughout the optimisation. The upper chain length is also fixed at 15 m, while the total mooring line length, polyester segment length, and initial horizontal pretension are treated as optimisation variables.

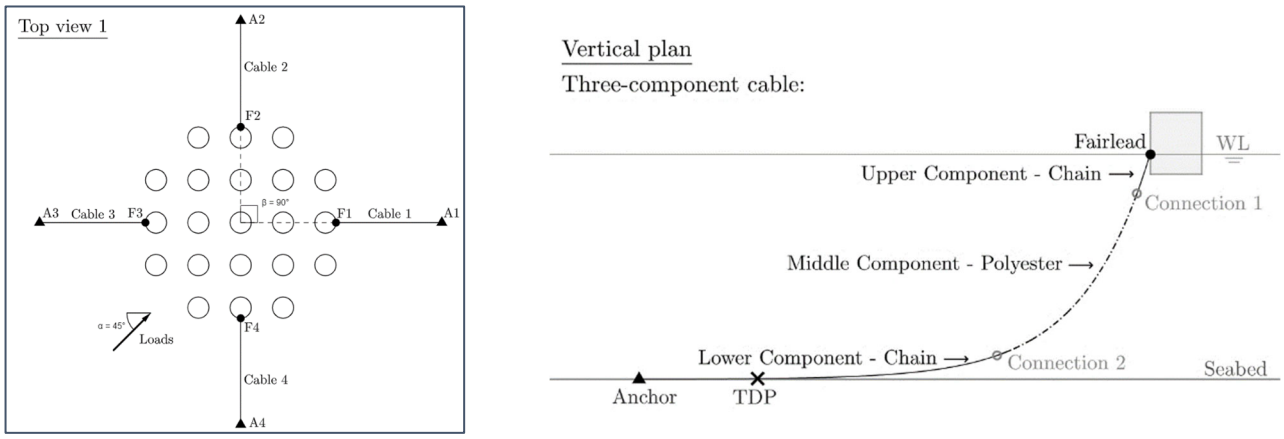

(a) **(b)**

Figure 4. Mooring configuration of the floating system (**a**) Top view; (**b**) Vertical view.

Table 1. Reference material properties.

Component	Property	Value
Chain	Type	R3 studless
	Nominal diameter	36 mm
	MBL	1189 kN
	Axial stiffness, EA	109.93 MN
	Dry mass per unit length	25.8 kg/m
Polyester rope	Nominal diameter	40 mm
	MBL	454 kN
	Axial stiffness, EA	4.59 MN
	Dry mass per unit length	1.12 kg/m
	Submerged mass per unit length	0.28 kg/m
Mooring system	Number of lines	4
	Upper chain length	15 m

3.2. Selected Sites and Environmental Conditions

The deployment sites considered in this study were derived from the GIS-based spatial screening conducted within Task 5.5 of the NATURSEA-PV project [23]. The assessment was applied to three representative European marine regions: the Algarve (Portugal), the Canary Islands (Spain), and the Adriatic Sea. The integrated resource availability, engineering and geological constraints, environmental protection, and marine spatial planning requirements were used to identify areas potentially suitable for OFPV deployment. Within the resulting areas, representative locations were defined to capture the spatial

variability in bathymetry and metocean conditions relevant to subsequent site-dependent mooring design and associated cost.

The complete screening assessment identified 16 representative locations in the Algarve, 19 in the Canary Islands, and 18 in the Adriatic Sea. For the present study, a subset of these locations is selected to cover a representative range of water depths and extreme environmental conditions for the mooring-cost analysis. The selected locations are shown in Figures 5–7, and their main characteristics are summarised in Tables 2–4.

Water depth and extreme metocean conditions constitute the principal site-specific inputs to the mooring analysis. Water depth directly influences the mooring-line geometry and required material length, while extreme waves and winds determine the environmental loading acting on the floating system. The 50-year return significant wave height $H_{s,50}$ and wind speed U_{50} are therefore used to characterise the extreme environmental conditions at each location. Distance to shore and annual Global Horizontal Irradiance (GHI) are also reported to provide broader context on the selected deployment sites, although they do not directly enter the mooring optimisation.

The selected sites encompass distinctly different deployment conditions. In the Algarve, water depths range from 63 to 304 m and $H_{s,50}$ from approximately 5.1 to 7.2 m. The Canary Islands sites span water depths of 76–220 m and $H_{s,50}$ of 3.9–6.9 m, together with the highest solar resource among the three regions. The Adriatic sites extend the analysis towards shallower and milder conditions, with water depths of 30–181 m and $H_{s,50}$ of approximately 2.4–4.5 m. Together, these locations provide a consistent range of site conditions for evaluating the influence of water depth and environmental severity on the optimised mooring configuration and associated material cost.

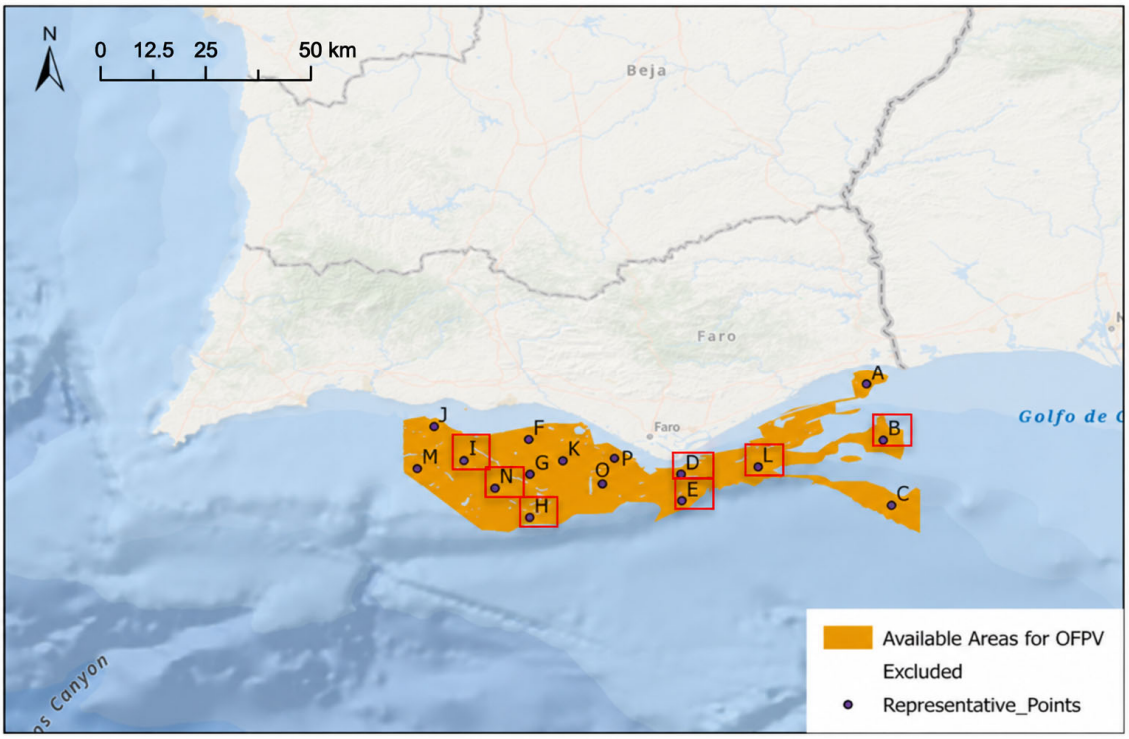

Figure 5. Selected reference points within potentially suitable OFPV areas in the Algarve.

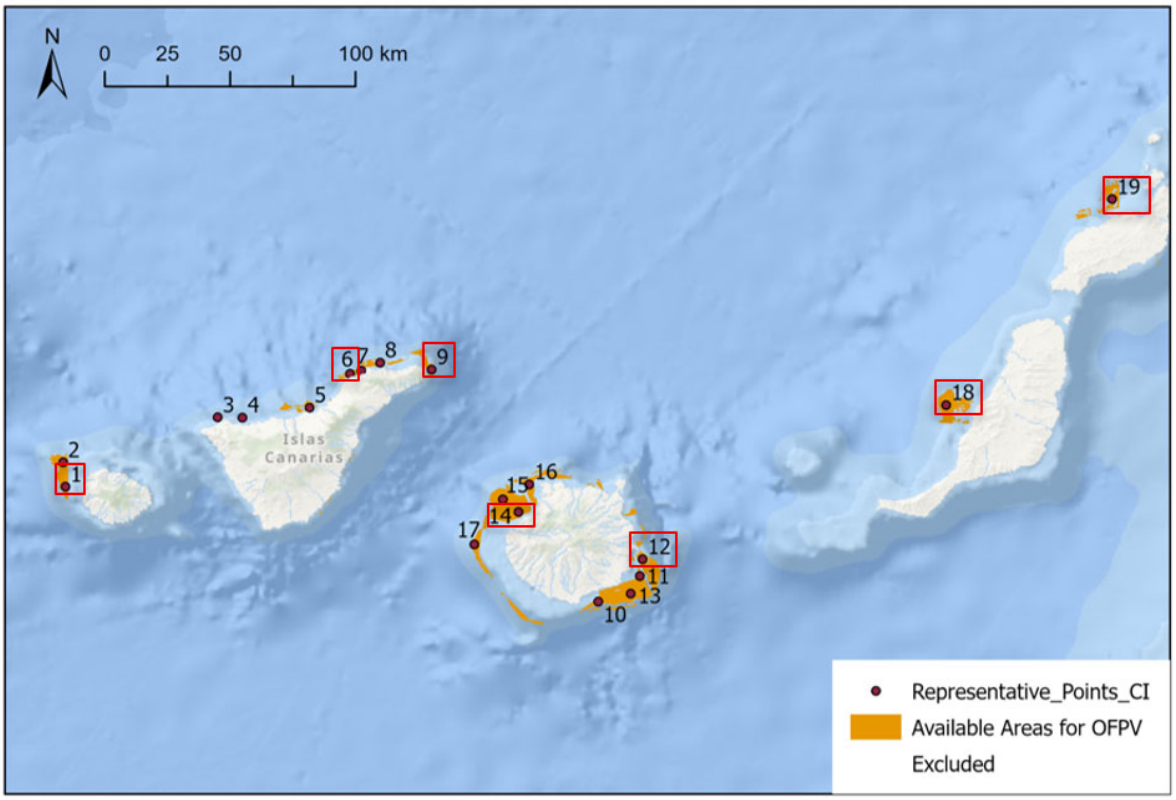

Figure 6. Selected reference points within potentially suitable OFPV areas in the Canary Islands.

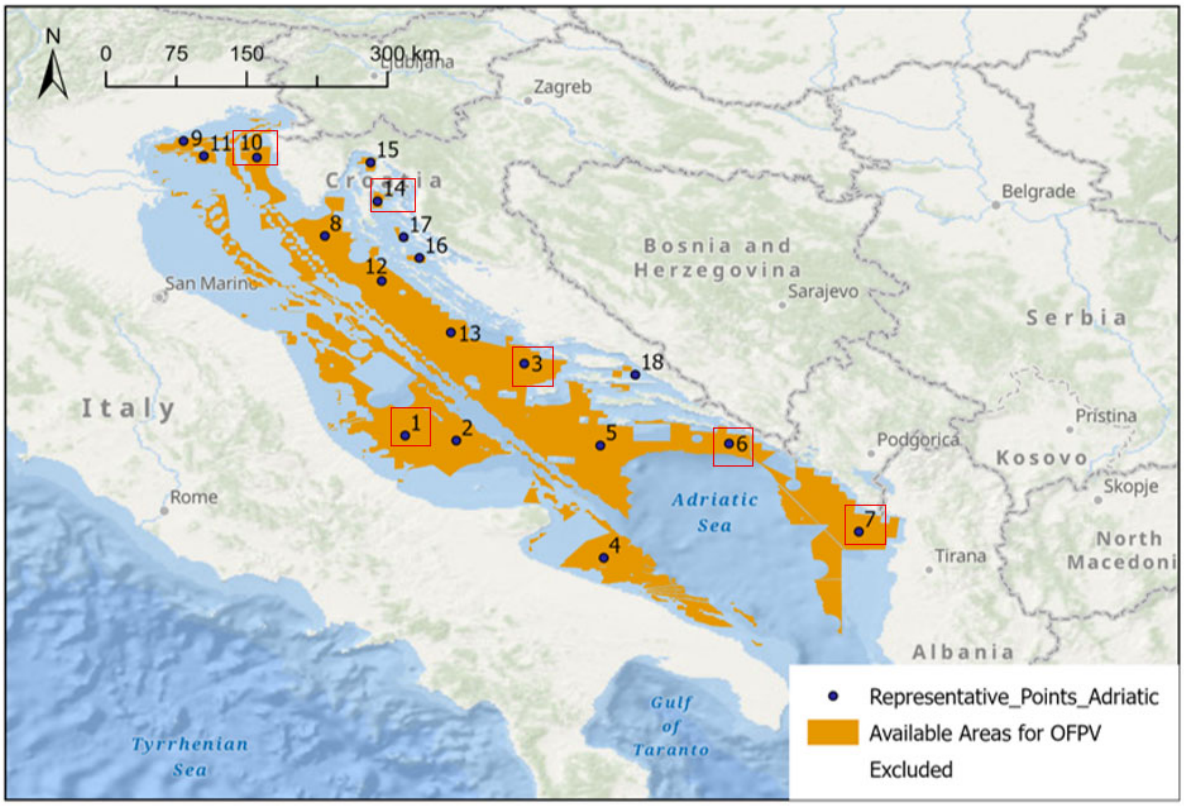

Figure 7. Selected reference points within potentially suitable OFPV areas in the Adriatic Sea.

Table 2. Selected sites and environmental conditions in the Algarve.

Site	Water Depth (m)	$H_{s,50\ (m)}$	$U_{w,50}$ (m/s)	Distance to Shore (km)	GHI (kWh/m^2/year)
I	63	5.36	21.15	11.61	1911
D	73	7.17	21.89	4.33	1917
N	96	7.24	20.80	16.67	1939
B	101	5.38	20.63	16.59	1919
H	132	7.24	20.81	24.19	1939
L	199	5.13	22.64	10.44	1917
E	304	7.17	20.85	11.21	1940

Table 3. Selected sites and environmental conditions in the Canary Islands.

Site	Water Depth (m)	$H_{s,50}$ (m)	$U_{w,50}$ (m/s)	Distance to Shore (km)	GHI (kWh/m^2/year)
C14	76	4.73	14.06	3.84	2069
C18	76	6.06	15.22	8.60	2072
C12	87	3.90	16.37	3.84	2116
C6	90	6.94	17.74	3.84	2028
C9	140	6.66	19.72	3.84	2002
C1	218	6.42	17.39	8.60	2173
C19	220	5.81	18.61	7.69	2021

Table 4. Selected sites and environmental conditions in the Adriatic Sea.

Site	Water Depth (m)	$H_{s,50}$ (m)	$U_{w,50}$ (m/s)	Distance to Shore (km)	GHI (kWh/m^2/year)
A10	30	3.63	18.66	14.57	1447
A14	94	2.37	18.04	7.28	1434
A7	94	4.22	19.94	21.85	1639
A3	124	3.92	20.32	16.29	1640
A1	177	4.51	22.30	41.20	1628
A6	181	4.06	19.03	14.57	1643

4. Results and Discussions

The optimization framework was applied to selected sites in the Algarve, Canary Islands and Adriatic Sea. The same chain and polyester material definitions and the same design constraints were used for both floating-platform designs. The results are first compared at platform level and then scaled to farm level. A farm contains 154 units for Design 1 and 84 units for Design 2.

4.1. Representative Comparison of the Two Platform Designs

Before comparing the optimised costs, a representative calculation at Site N (water depth 96 m) is used to confirm that the specific environmental loads and dynamic response are evaluated separately for the two designs. The same reference mooring configuration is used in this comparison so that the effect of the platform properties could be isolated.

Table 5 compares the environmental loads and mooring responses of the two designs at Site N using the same mooring line configuration. Design 2 has a slightly larger total mean environmental force of 11.737 kN compared with 10.276 kN for Design 1. The current force increases from 1.100 kN for Design 1 to 1.615 kN for Design 2 due to the larger draft and the corresponding difference in the projected geometry. The wind forces are relatively similar, with values of 8.412 kN and 7.932 kN for Designs 1 and 2, respectively. A more significant difference is observed for the mean wave drift force, which increases from 0.764 kN for Design 1 to 2.190 kN for Design 2 due to the different hydrodynamic characteristics of the two platforms.

Table 5. Comparison of the environmental loads and mooring responses of the two designs at Site N.

Parameter	Design 1	Design 2
Body mass (kg)	123,200.3	283,500.0
Current force (kN)	1.100	1.615
Wind force (kN)	8.412	7.932
Mean wave drift force (kN)	0.764	2.190
Total mean force (kN)	10.276	11.737
Mean offset (m)	1.4154	1.6156
Dynamic surge amplitude (m)	2.5416	1.1972
Maximum offset (m)	3.9569	2.8128
Maximum fairlead tension (kN)	42.263	38.247
Maximum tension/MBL	0.09309	0.08424
Anchor radius (m)	237.858	247.988

The larger mean environmental force results in a moderately higher mean offset for Design 2, increasing from 1.4154 m to 1.6156 m. However, the dynamic surge amplitude of Design 2 is considerably smaller, decreasing from 2.5416 m to 1.1972 m. This difference is mainly associated with the larger inertia of Design 2. Its body mass is 283.5 t compared with 123.2 t for Design 1, while the hydrodynamic analysis also indicates a larger surge added mass. Although the wave excitation force of Design 2 is not necessarily smaller, the increased total inertia reduces the wave frequency surge response.

Consequently, the maximum offset decreases from 3.9569 m for Design 1 to 2.8128 m for Design 2. The corresponding maximum fairlead tension also decreases from 42.263 kN to 38.247 kN. These results indicate that the larger mean environmental load of Design 2 does not directly lead to a larger maximum mooring response, since the dynamic contribution to the surge motion is significantly reduced.

4.2. Optimized Mooring Results for Design 1

The farm-level cost is calculated independently from the optimised cost of one floating unit as $C_{farm} = 154 \times C_{unit}$. The reported unit costs in Tables 6–8 include the chain, polyester rope, and estimated anchor costs used in the optimisation model.

Table 6. Summary of the cost estimation for Design 1 at Algarve sites.

Site	h (m)	L_{tot} (m)	L_{poly} (m)	L_{bottom} (m)	H_0/MBL	T_{max}/MBL	Offset/h	Unit Cost (USD)	Farm Cost (MUSD)
I	63	138.8	95.4	28.4	0.0305	0.108	0.034	18,431	2.838
D	73	175.7	122.1	38.5	0.0305	0.109	0.052	21,606	3.327
N	96	211.5	145.4	51.1	0.0305	0.070	0.044	23,271	3.584
B	101	222.5	153.0	54.5	0.0305	0.057	0.030	23,686	3.648
H	132	290.8	199.9	75.9	0.0305	0.063	0.035	30,436	4.687
L	199	438.4	301.4	122.0	0.0305	0.059	0.023	44,259	6.816
E	304	669.8	460.5	194.3	0.0305	0.061	0.020	66,414	10.228

Table 7. Summary of the cost estimation for Design 1 at the Canary Islands.

Site	h (m)	L_{tot} (m)	L_{poly} (m)	L_{bottom} (m)	H_0/MBL	T_{max}/MBL	Offset/h	Unit Cost (USD)	Farm Cost (MUSD)
C14	76	190.0	132.9	42.1	0.0305	0.055	0.025	20,019	3.083
C18	76	190.0	132.9	42.1	0.0305	0.059	0.030	20,249	3.118
C12	87	217.5	152.1	50.4	0.0305	0.051	0.019	22,388	3.448
C6	90	225.0	157.3	52.7	0.0305	0.065	0.037	23,746	3.657
C9	140	308.4	212.1	81.4	0.0305	0.060	0.029	31,936	4.918
C1	218	480.3	330.2	135.1	0.0305	0.056	0.018	48,140	7.414
C19	220	484.7	333.2	136.5	0.0305	0.056	0.018	48,541	7.475

Table 8. Summary of the cost estimation for Design 1 at Adriatic Sea.

Site	h (m)	L_{tot} (m)	L_{poly} (m)	L_{bottom} (m)	H_0/MBL	T_{max}/MBL	Offset/h	Unit Cost (USD)	Farm Cost (MUSD)
A10	30	90.0	62.9	12.1	0.0366	0.089	0.020	12,762	1.965
A14	94	207.1	142.4	49.7	0.0305	0.049	0.017	21,836	3.363
A7	94	207.1	142.4	49.7	0.0305	0.056	0.027	22,134	3.409
A3	124	273.2	187.8	70.4	0.0305	0.054	0.023	28,347	4.365
A1	177	390.0	268.1	106.9	0.0305	0.058	0.023	39,610	6.100
A6	181	398.8	274.2	109.6	0.0305	0.054	0.018	40,283	6.204

For Design 1, Site A10 is represented by the completed feasible solution from the Adriatic optimisation summary results. The completed optimisation gives L_{tot} = 90.0 m, L_{poly} = 62.9 m, T_{max}/MBL = 0.089, offset/h = 0.020 and a unit mooring cost of approximately USD 12,762.

4.3. Optimized Mooring Results for Design 2

The farm level cost is calculated independently from the optimised cost of one floating unit as C_{farm} = 84 C_{unit}. The reported unit cost in Tables 9–11 includes the chain, polyester rope and estimated anchor costs used in the optimisation model.

Table 9. Summary of the cost estimation for Design 2 at Algarve sites.

Site	h (m)	L_{tot} (m)	L_{poly} (m)	L_{bottom} (m)	H_0/MBL	T_{max}/MBL	Offset/h	Unit Cost (USD)	Farm Cost (MUSD)
I	63	157.5	109.5	33.0	0.0305	0.063	0.028	17,604	1.479
D	73	182.5	126.9	40.6	0.0305	0.065	0.035	20,031	1.683
N	96	240.0	167.8	57.2	0.0344	0.063	0.027	25,037	2.103
B	101	227.2	156.2	56.0	0.0327	0.057	0.025	24,149	2.029
H	132	297.0	204.2	77.8	0.0327	0.060	0.026	30,915	2.597
L	199	447.8	307.8	124.9	0.0327	0.060	0.020	45,221	3.799
E	304	684.0	470.2	198.8	0.0327	0.061	0.017	67,809	5.696

Table 10. Summary of the cost estimation for Design 2 at the Canary Islands.

Site	h (m)	L_{tot} (m)	L_{poly} (m)	L_{bottom} (m)	H_0/MBL	T_{max}/MBL	Offset/h	Unit Cost (USD)	Farm Cost (MUSD)
C14	76	190.0	132.1	42.9	0.0305	0.049	0.017	19,914	1.673
C18	76	190.0	132.1	42.9	0.0305	0.053	0.022	20,100	1.688
C12	87	217.5	152.1	50.4	0.0344	0.053	0.015	22,455	1.886
C6	90	225.0	156.4	53.6	0.0305	0.056	0.025	23,513	1.975
C9	140	315.0	216.6	83.4	0.0327	0.059	0.023	32,539	2.733
C1	218	490.5	337.2	138.3	0.0327	0.057	0.016	49,178	4.131
C19	220	495.0	340.3	139.7	0.0327	0.057	0.016	49,622	4.168

Table 11. Summary of the cost estimation for Design 2 at Adriatic Sea.

Site	h (m)	L_{tot} (m)	L_{poly} (m)	L_{bottom} (m)	H_0/MBL	T_{max}/MBL	Offset/h	Unit Cost (USD)	Farm Cost (MUSD)
A10	30	90.0	62.9	12.1	0.0366	0.076	0.015	12,079	1.015
A14	94	235.0	164.3	55.7	0.0305	0.048	0.014	23,832	2.002
A7	94	235.0	164.3	55.7	0.0305	0.052	0.019	24,008	2.017
A3	124	279.0	191.8	72.2	0.0307	0.053	0.020	28,861	2.424
A1	177	398.2	273.8	109.5	0.0307	0.056	0.020	40,350	3.389
A6	181	407.2	280.0	112.3	0.0307	0.053	0.016	41,074	3.450

4.4. Cost Comparison Between Design 1 and Design 2

At the individual platform level, the optimised mooring costs of the two designs are generally close. This is consistent with the representative response comparison. Although the environmental loads differ, the governing maximum offset and line tension can remain similar because the mean and dynamic response components change differently between the two platforms. The differences in the cost between the two designs are listed in Table 12.

Table 12. Comparison of the results between Design 1 and Design 2.

Region	Site	D1 Unit (USD)	D2 Unit (USD)	Unit Diff.	D1 Farm (MUSD)	D2 Farm (MUSD)	Farm Diff.
Algarve	I	18,431	17,604	−4.5%	2.838	1.479	−47.9%
Algarve	D	21,606	20,031	−7.3%	3.327	1.683	−49.4%
Algarve	N	23,271	25,037	+7.6%	3.584	2.103	−41.3%
Algarve	B	23,686	24,149	+2.0%	3.648	2.029	−44.4%
Algarve	H	30,436	30,915	+1.6%	4.687	2.597	−44.6%
Algarve	L	44,259	45,221	+2.2%	6.816	3.799	−44.3%
Algarve	E	66,414	67,809	+2.1%	10.228	5.696	−44.3%
Canary	C14	20,019	19,914	−0.5%	3.083	1.673	−45.7%
Canary	C18	20,249	20,100	−0.7%	3.118	1.688	−45.9%
Canary	C12	22,388	22,455	+0.3%	3.448	1.886	−45.3%
Canary	C6	23,746	23,513	−1.0%	3.657	1.975	−46.0%
Canary	C9	31,936	32,539	+1.9%	4.918	2.733	−44.4%
Canary	C1	48,140	49,178	+2.2%	7.414	4.131	−44.3%
Canary	C19	48,541	49,622	+2.2%	7.475	4.168	−44.2%
Adriatic	A10	12,762	12,079	−5.4%	1.965	1.015	−48.4%
Adriatic	A14	21,836	23,832	+9.1%	3.363	2.002	−40.5%
Adriatic	A7	22,134	24,008	+8.5%	3.409	2.017	−40.8%
Adriatic	A3	28,347	28,861	+1.8%	4.365	2.424	−44.5%
Adriatic	A1	39,610	40,350	+1.9%	6.100	3.389	−44.4%
Adriatic	A6	40,283	41,074	+2.0%	6.204	3.450	−44.4%

Across the comparable feasible sites, the mean increase in unit-level cost from Design 1 to Design 2 is about 0.5% in the Algarve, 0.6% in the Canary Islands and 3.0% in the Adriatic Sea. The largest increases occur at the two 94 m Adriatic sites (A14 and A7), where the unit cost of Design 2 is approximately 8–9% higher. In contrast, Site D in the Algarve gives a slightly lower optimised unit cost for Design 2, reflecting the discrete change in the selected line-length ratios rather than a simple monotonic scaling with platform size.

The farm level comparison is substantially different because the number of floating units is not the same. Design 1 requires 154 units, whereas Design 2 requires only 84 units. The mooring system of one Design 2 unit could be approximately 83% more expensive than that of Design 1 before the two farm-level mooring costs become equal. In the present results, the unit cost differences are far below this threshold. Consequently, the calculated Design 2 farm level mooring cost is approximately 40–49% lower than Design 1 across the directly comparable sites.

As expected, water depth is the dominant parameter determining the optimised material cost in the present dataset. Deeper sites require longer total mooring lines and larger polyester and bottom-chain lengths, leading to a strong increase in cost. Environmental severity still affects tension utilisation, offset and the detailed optimum, but its influence on cost is secondary to the geometric requirement imposed by water depth for the fixed material system considered here. This trend is visible consistently in all three regions. The present farm costs should be interpreted as comparative mooring system estimates rather than complete life-cycle costs. They include the line materials and estimated anchors used in the optimisation model, but exclude installation vessels, connectors and hardware not explicitly modelled, inspection,

maintenance and decommissioning. These additional cost components may affect both the absolute costs and the relative economic performance of the two designs and should be considered in a more comprehensive techno-economic assessment.

Figure 8 shows a strong increase in optimised unit cost with water depth for both platform designs. This behaviour follows directly from the longer total line, polyester, and bottom-chain segments required in deeper water. Based on the data presented in Figure 8, the Pearson correlation between water depth and unit cost is 0.997 for Design 1 and 0.999 for Design 2. The corresponding correlations between total line length and cost are 0.998 and 0.999, respectively.

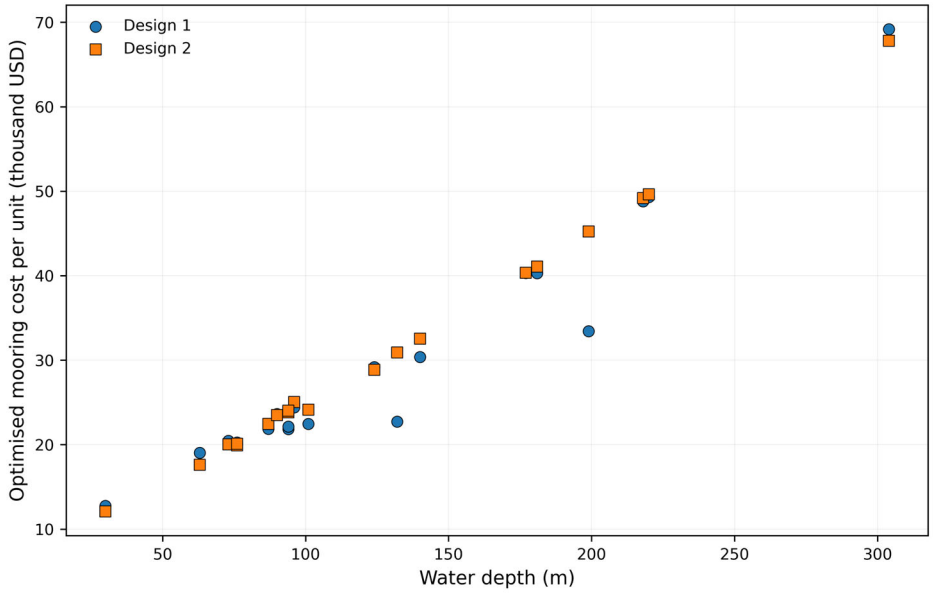

Figure 8. Optimised mooring cost per floating unit as a function of water depth.

Figure 9 compares the farm-level mooring cost at sites for which feasible results are available for both designs. Although Design 2 generally has a slightly higher cost per floating unit, the lower number of units required in the farm (84 instead of 154) dominates the farm-level comparison. Consequently, Design 2 gives a lower farm mooring cost at every directly comparable site in the present dataset.

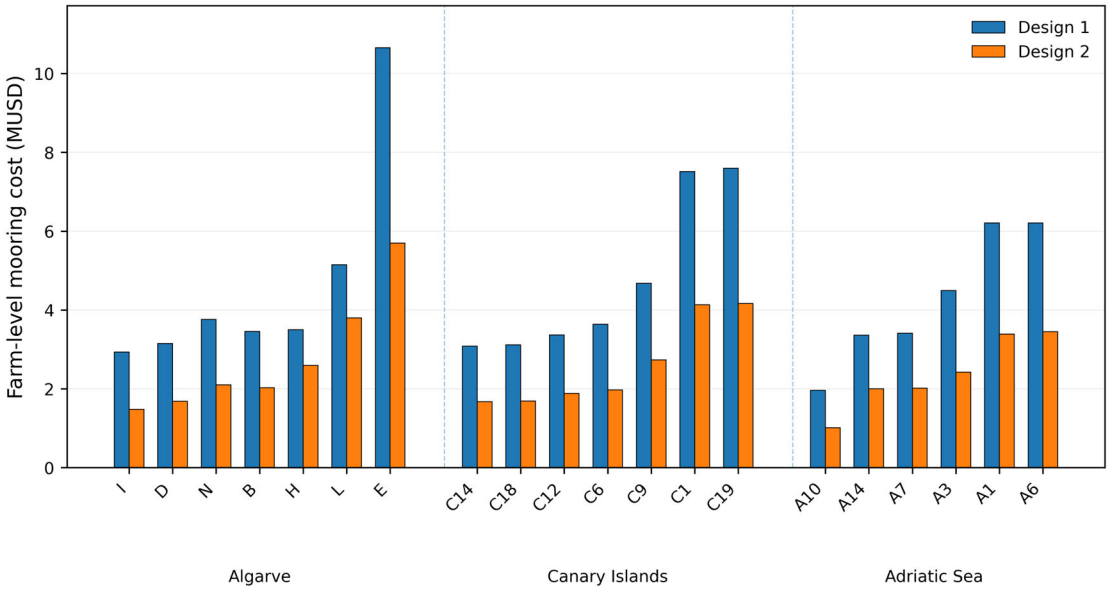

Figure 9. Farm-level mooring cost comparison for Design 1 and Design 2.

Figure 10 highlights the different conclusions obtained at the two comparison scales. The unit cost of Design 2 varies only moderately relative to Design 1, whereas the farm-level difference remains strongly negative because of the reduced number of floating units. The unit mooring cost of Design 2 ranges from 7.3% lower to 9.1% higher than that of Design 1 across the selected sites, while the farm-level cost is 40.5% to 49.4% lower than Design 1. This confirms that unit level mooring cost alone is not an adequate indicator for comparing the two floating-solar farm concepts.

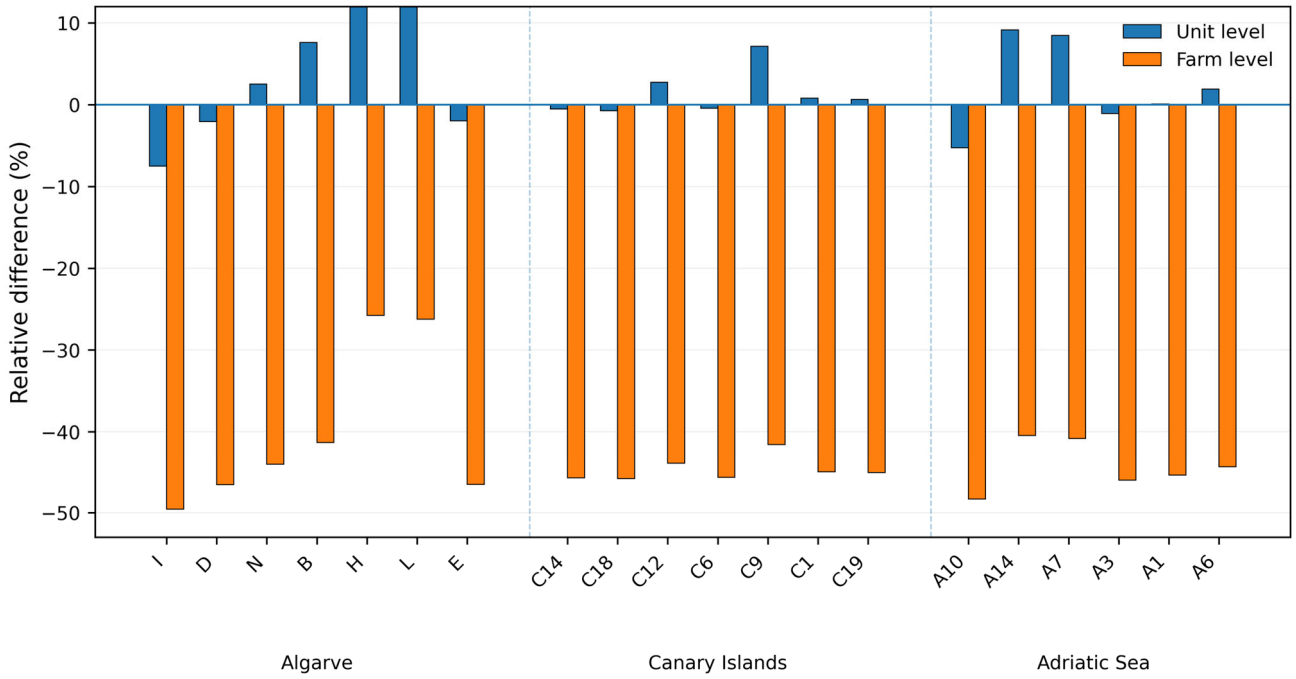

Figure 10. Relative Design 2 cost difference compared with Design 1 at unit and farm levels.

As shown in Table 13, sites at the same water depth provide a useful check of the role of environmental severity because the basic geometric requirement of the mooring system is unchanged. The dataset includes two representative pairs: C14/C18 at 76 m water depth and A14/A7 at 94 m. In both cases, the site with the larger significant wave height develops higher tension utilisation and offset, whereas the optimised cost changes only slightly. This supports the interpretation that environmental conditions influence the response constraints and detailed optimum, while water depth remains the dominant driver of material quantity and cost.

Table 13. Comparison of the results of Design 1 and Design 2 for different sites with similar water depth.

Design	Region	Sites	h (m)	$H_{s,50}$ (m)	T_{max}/MBL	Offset/h	Unit Cost (USD)
Design 1	Canary Islands	C14 *vs.* C18	76	4.73/6.06	0.055/0.059	0.025/0.030	20,019/20,249
Design 1	Adriatic Sea	A14 *vs.* A7	94	2.37/4.22	0.049/0.056	0.017/0.027	21,836/22,134
Design 2	Canary Islands	C14 *vs.* C18	76	4.73/6.06	0.049/0.053	0.017/0.022	19,914/20,100
Design 2	Adriatic Sea	A14 *vs.* A7	94	2.37/4.22	0.048/0.052	0.014/0.019	23,832/24,008

5. Conclusions

This study investigates the site dependent mooring design and associated mooring material costs of two offshore floating photovoltaic platform concepts at 20 selected sites across the Algarve, Canary Islands and Adriatic Sea. A three-component chain-polyester-chain mooring system is optimised for both designs considering line tension, platform offset, and seabed clearance constraints, using a quasi-static method. The total mooring line length, polyester segment length and initial pretension are considered as design variables. The resulting mooring configurations and costs were compared at both the individual floating unit and farm levels.

The results show that the optimised mooring cost is determined primarily by water depth and the associated line length requirement. Across the selected sites, the correlation coefficients between water depth and unit mooring cost are 0.997 and 0.999 for Designs 1 and 2, respectively, while the corresponding correlations between total line length and cost are 0.998 and 0.999. Differences in wave and wind conditions are clearly reflected in line tension and platform offset but produce much smaller cost changes when the water depth and selected line geometry are similar. Despite the differences in environmental loads and dynamic responses, the two platform designs therefore lead to broadly comparable mooring costs per floating unit. Across the directly comparable sites, the unit cost of Design 2 varies from 7.3% lower to 9.1% higher than that of Design 1. At farm level, however, Design 2 requires only 84 floating units compared with 154 units for Design 1. This difference dominates the farm level comparison, resulting in a 40.5–49.4% reduction in the estimated farm level mooring cost for Design 2.

The present comparison is limited to the optimised mooring lines and estimated anchor costs and does not represent the complete farm CAPEX. Installation, connectors and other hardware, inspection, maintenance and decommissioning costs are not included. Nevertheless, the results demonstrate the importance of considering both site dependent mooring requirements and the number of floating units when comparing alternative OFPV concepts at farm level. The developed approach provides a direct link between mooring design and farm scale cost assessment and can support subsequent techno-economic and LCOE evaluations of offshore floating photovoltaic systems.

Statement of the Use of Generative AI and AI-Assisted Technologies in the Writing Process

During the preparation of this manuscript, the authors used ChatGPT in order to polish the language of the manuscript. After using this tool/service, the authors reviewed and edited the content as needed and take(s) full responsibility for the content of the published article.

Acknowledgement

This work has been supported by the project “Novel eco-cementitious materials and components for durable, competitive, and bio-inspired offshore floating PV substructures (NaturSea-PV)”, funded by the Horizon Europe Programme of the European Union under contract number GA nº 101084348. However, the views and opinions expressed are those of the author(s) only and do not necessarily reflect those of the European Union or the European Climate Infrastructure and Environment Executive Agency (CINEA). Neither the European Union nor the granting authority can be held responsible for them. This work contributes to the Strategic Research Plan of the Centre for Marine Technology and Ocean Engineering (CENTEC), which is financed by the Portuguese Foundation for Science and Technology (Fundação para a Ciência e Tecnologia—FCT) under contract UID/00134/2025 (https://doi.org/10.54499/UID/00134/2025) (accessed on 24 November 2026).

Author Contributions

Conceptualization, S.W.; Methodology, S.W., H.J. and A.S.; Software, H.J. and A.S.; Validation, S.W., H.J., A.S. and S.R.-M.; Formal Analysis, S.W., H.J., A.S. and S.R.-M.; Investigation, S.W., H.J., A.S. and S.R.-M.; Resources, C.G.S.; Data Curation, S.W., H.J., A.S. and S.R.-M.; Writing—Original Draft Preparation, S.W., H.J., A.S., S.R.-M. and C.G.S.; Writing—Review & Editing, S.W., H.J., A.S., S.R.-M. and C.G.S.; Visualization, S.W., H.J., A.S. and S.R.-M.; Supervision, S.W. and C.G.S.; Project Administration, C.G.S.; Funding Acquisition, C.G.S.

Ethics Statement

Not applicable.

Informed Consent Statement

Not applicable.

Data Availability Statement

The statement is required for all original articles which informs readers about the accessibility of research data linked to a paper and outlines the terms under which the data can be obtained.

Funding

This research was funded by the European Union's Horizon Europe Programme grant number 101084348 and the Portuguese Foundation for Science and Technology (FCT) grant number UID/00134/2025 (https://doi.org/10.54499/UID/00134/2025.

Declaration of Competing Interest

The authors declare that they have no known competing financial interests or personal relationships that could have appeared to influence the work reported in this paper.

References

1. Sahu A, Yadav N, Sudhakar K. Floating photovoltaic power plant: A review. *Renew. Sustain. Energy Rev.* **2016**, *66*, 815–824. DOI:10.1016/j.rser.2016.08.051
2. Oliveira-Pinto S, Stokkermans J. Marine floating solar plants: An overview of potential, challenges and feasibility. *Proc. Inst. Civ. Eng. Marit. Eng.* **2020**, *173*, 120–135. DOI:10.1680/jmaen.2020.10
3. Clemente G, Ramos-Marin S, Guedes Soares C. Overview of the Floating Offshore Photovoltaic Energy Potential. In *Advances in Maritime Technology and Engineering*; Guedes Soares C, Santos TA, Eds.; Taylor and Francis: London, UK, 2024; pp. 417–425. DOI:10.1201/9781003508779-45
4. Claus R, López M. Key issues in the design of floating photovoltaic structures for the marine environment. *Renew. Sustain. Energy Rev.* **2022**, *164*, 112502. DOI:10.1016/j.rser.2022.112502
5. Yu F, Su Y, Liu Y, Liu H, Duan F. Dynamic response of the mooring system in the floating photovoltaic power station. *J. Phys. Conf. Ser.* **2021**, *2087*, 012028. DOI:10.1088/1742-6596/2087/1/012028
6. Ghigo A, Faraggiana E, Sirigu M, Mattiazzo G, Bracco G. Design and analysis of a floating photovoltaic system for offshore installation: The case study of Lampedusa. *Energies* **2022**, *15*, 8804. DOI:10.3390/en15238804
7. Weller SD, Johanning L, Davies P, Banfield SJ. Synthetic mooring ropes for marine renewable energy applications. *Renew. Energy* **2015**, *83*, 1268–1278. DOI:10.1016/j.renene.2015.03.058
8. Xu S, Wang S, Guedes Soares C. Review of mooring design for floating wave energy converters. *Renew. Sustain. Energy Rev.* **2019**, *111*, 595–621. DOI:10.1016/j.rser.2019.05.027
9. Xu S, Wang S, Guedes Soares C. Experimental study of the influence of the rope material on mooring fatigue damage and point absorber response. *Ocean Eng.* **2021**, *232*, 108667. DOI:10.1016/j.oceaneng.2021.108667
10. Han H, Du Z, Ma G, Fu Q, Zhang C. Integrated coupling analysis and multi-objective optimization of mooring system for floating photovoltaic arrays. *Ocean Eng.* **2025**, *333*, 121536. DOI:10.1016/j.oceaneng.2025.121536
11. Striani R, Jiang H, Biroli MV, Shao Y, Wang S. Review of Floating Offshore Wind Turbines with Shared Mooring Systems. *J. Mar. Sci. Eng.* **2025**, *13*, 2341. DOI:10.3390/jmse13122341
12. Thomsen JB, Ferri F, Kofoed JP, Black K. Cost optimization of mooring solutions for large floating wave energy converters. *Energies* **2018**, *11*, 159. DOI:10.3390/en11010159
13. Housner S, Hall M, Tran TT, de Miguel Para B, Maeso A. Shared mooring system designs and cost estimates for wave energy arrays. *Renew. Energy* **2024**, *231*, 120924. DOI:10.1016/j.renene.2024.120924
14. Castro-Santos L, Martins E, Guedes Soares C. Methodology to calculate the costs of a floating offshore renewable energy farm. *Energies* **2016**, *9*, 324. DOI:10.3390/en9050324
15. Castro-Santos L, Silva D, Bento AR, Salvação N, Guedes Soares C. Economic feasibility of floating offshore wind farms in Portugal. *Ocean Eng.* **2020**, *207*, 107393. DOI:10.1016/j.oceaneng.2020.107393
16. Myhr A, Bjerkseter C, Ågotnes A, Nygaard TA. Levelised cost of energy for offshore floating wind turbines in a life cycle perspective. *Renew. Energy* **2014**, *66*, 714–728. DOI:10.1016/j.renene.2014.01.017

17. Lerch M, De-Prada-Gil M, Molins C, Benveniste G. Sensitivity analysis on the levelized cost of energy for floating offshore wind farms. *Sustain. Energy Technol. Assess.* **2018**, *30*, 77–90. DOI:10.1016/j.seta.2018.09.005
18. Martinez A, Iglesias G. Mapping of the levelised cost of energy from floating solar PV in coastal waters of the European Atlantic, North Sea and Baltic Sea. *Sol. Energy* **2024**, *279*, 112809. DOI:10.1016/j.solener.2024.112809
19. Bru J, Seland TS, Dai J, Jiang Z. Life cycle cost analysis of an offshore floating photovoltaic concept in the North Sea. *Renew. Energy* **2025**, *249*, 122981. DOI:10.1016/j.renene.2025.122981
20. NATURSEA PV, 2025. D1.5—Mooring Concepts. NATURSEA PV Project, Deliverable D1.5.
21. Desiderati J, Vidal FJ, Biroli MV, Wang S, Guedes Soares C, Baderiya N, et al. Mooring design and analysis for a floating solar system. In Proceedings of the 6th International Conference on Renewable Energies Offshore (RENEW 2024), Lisbon, Portugal, 19–21 November 2024; pp. 389–400. DOI:10.1201/9781003558859-43
22. Wang S, Desiderati J, Guedes Soares C. Dynamic analysis of mooring lines and a floating offshore photovoltaic system under extreme environmental conditions. In Proceedings of the ASME 2026 45th International Conference on Ocean, Offshore and Arctic Engineering (OMAE2026), Tokyo, Japan, 7–12 June 2026; Paper No. OMAE2026-174368. DOI:10.1115/OMAE2026-174368
23. Ramos-Marin S, Abdelghany GA, Guedes Soares C. Geospatial Site Screening for Offshore Floating Photovoltaic Deployment in the Adriatic Sea. In *Advances in Maritime Technology and Engineering*; Guedes Soares C, Salvado FC, Eds.; Taylor and Francis: London, UK, 2026. DOI:10.1201/9781042001194-142.
24. Abdelghany GA, Guedes Soares C. Environmental Conditions for Deploying Offshore Floating Solar Photovoltaic Energy Installations. In *Innovations in Renewable Energies Offshore*; Guedes Soares C, Wang S, Eds.; Taylor and Francis: London, UK, 2025; pp. 107–118. DOI:10.1201/9781003558859-13
25. Bergdahl L, Kofoed JP. *Simplified Design Procedures for Moorings of Wave-Energy Converters: Deliverable 2.2*; DCE Technical Reports No. 172; Department of Civil Engineering, Aalborg University: Aalborg, Denmark, 2015.
26. Depalo F, Wang S, Xu S, Guedes Soares C. Design and analysis of a mooring system for a wave energy converter. *J. Mar. Sci. Eng.* **2021**, *9*, 782. DOI:10.3390/jmse9070782
27. *DNVGL-OS-E301*; Position Mooring. Offshore Standard, Edition July 2018; DNV GL AS: Høvik, Norway, 2018.
28. *DNVGL-RP-C205*; Environmental Conditions and Environmental Loads. Recommended Practice, Edition September 2019; DNV GL AS: Høvik, Norway, 2019.
29. Audet C, Dennis JE, Jr. Analysis of generalized pattern searches. *SIAM J. Optim.* **2003**, *13*, 889–903. DOI:10.1137/S1052623400378742
30. Baderiya N, Otto W, Camacho E, Abdelghany G, Wang S, Guedes Soares C. Conceptual design of an offshore photovoltaic system in low-carbon ultra-high-performance concrete. In Proceedings of the ASME 2026 45th International Conference on Ocean, Offshore and Arctic Engineering (OMAE2026), Tokyo, Japan, 7–12 June 2026; Paper No. OMAE2026-183573. DOI:10.1115/OMAE2026-183573
31. Camacho E. D1.3—Structural Design of the Components. NATURSEA-PV Project, Deliverable D1.3, Horizon Europe Project No. 101084348. 2025.
32. Chakrabarti SK. *Handbook of Offshore Engineering*; Elsevier: Oxford, UK, 2005.
33. Bridon. Fibre Rope Catalogue. https://www.yumpu.com/en/document/view/33598438/fibre-rope-catalogue-bridon (accessed on 21 November 2026).